All-optical switching at the Fano resonances in subwavelength gratings with very narrow slits

G. D'Aguanno,[1,2,*] D. de Ceglia,[1,2] N. Mattiucci,[1,2] and M. J. Bloemer[2]

[1]*Nanogenesis Division, AEgis Technologies, 410 Jan Davis Drive, Huntsville, Alabama 35806, USA*

[2]*Charles M. Bowden Laboratory, Building 7804, Redstone Arsenal, Huntsville, Alabama 35898, USA*

**Corresponding author: giuseppe.daguanno@us.army.mil*

Received March 18, 2011; revised April 19, 2011; accepted April 20, 2011;
posted April 26, 2011 (Doc. ID 144429); published May 23, 2011

We theoretically discuss all-optical switching at the Fano resonances of subwavelength gratings made of a chalcogenide glass (As_2S_3). Particular attention is devoted to the case in which the grating possesses extremely narrow slits (channels ranging from $a \sim 10$ nm to $a \sim 40$ nm). The remarkable local field enhancement available in these situations conspires to yield low-threshold switching intensities ($\sim 50\,MW/cm^2$) at telecommunication wavelengths for extremely thin ($d \sim 200$ nm) gratings when a realistic value of the As_2S_3 cubic nonlinearity is used.

OCIS codes: 050.6624, 190.1450, 190.3270.

All-optical switching devices are based on the optical Kerr effect in which the local refractive index of the material is linearly modified with the intensity of the field [1]: $n = n_L + n_2 I$, n_L is the linear refractive index of the material, n_2 is the nonlinear refraction coefficient, and I the local field intensity. The nonlinear refraction index n_2 and the two photon absorption (TPA) coefficient β can also be related, respectively, to the real and imaginary parts of the cubic $\chi^{(3)}$ nonlinearity through the following relations [2]: $\mathrm{Re}[\chi^{(3)}] = \varepsilon_0 c n_L^2 n_2$ and $\mathrm{Im}[\chi^{(3)}] = \varepsilon_0 c n_L^2 \lambda\beta/(4\pi)$, where ε_0 is the vacuum permittivity, c the speed of light *in vacuo*, and λ the wavelength. In [3] was demonstrated that all-optical switching can be possible only when the following relation is satisfied: $(\mathrm{Im}[\chi^{(3)}]/\mathrm{Re}[\chi^{(3)}]) < 1/(8\pi)$ or, equivalently, a figure of merit (FOM) $\mathrm{FOM} = n_2/(2\beta\lambda) > 1$. For example, in the case of GaAs we can extrapolate n_2 and β at $\lambda \sim 1.5\,\mu$m using experimental data available in the literature [4] from which we obtain an $\mathrm{FOM} = 0.066$ preventing obviously any all-optical switching according to the criterion laid out in [3]. Among alternative materials for all-optical signal processing, chalcogenide glasses stand out due to their large, ultrafast third-order nonlinearities and low TPA [5]. The aim of this Letter is to show that it is possible to achieve all-optical switching at extremely low input intensity ($\sim 50\,MW/cm^2$) by using the Fano resonances [6] available in a diffraction grating. In particular, we use a diffraction grating made of As_2S_3 (arsenic trisulfide), which belongs to the family of the chalcogenide glasses [5], for the reasons mentioned above. While the idea to use the sharp resonances available in a diffraction grating for optical bistable devices dates back to almost three decades ago [7], in this Letter we will analyze in particular the regime of diffraction gratings with extremely narrow slits whose apertures a range from $a \sim 10$ nm to $a \sim 40$ nm. Structures like the ones we propose here might nowadays be fabricated using advanced nanofabrication techniques [8]. In general, Fano resonances originate in any quantum or classical system that admits discrete states (be they the quantum eigenstates of an atomic system or the guided modes of a waveguide, for example) coupled with continuum states (be they the Breit-Wigner resonances of an excited atom or the transmission resonances of a Fabry–Perot etalon, for example). The reader interested in a more detailed account of the role of Fano resonances in many physical systems can consult [9,10]. The linear properties of Fano resonances in chalcogenide photonic crystal membranes have been studied in [11], for example. In our case, Fano resonances can be simply obtained by using a subwavelength grating as the one shown in Fig. 1(a). Fano resonances will in this case be generated by the coupling of the continuum Fabry–Perot etalon resonances of the unperturbed (no grating) air/As_2S_3/substrate structure along z with the discrete guided modes admitted by the same unperturbed structure air/As_2S_3/substrate along the x direction, as also

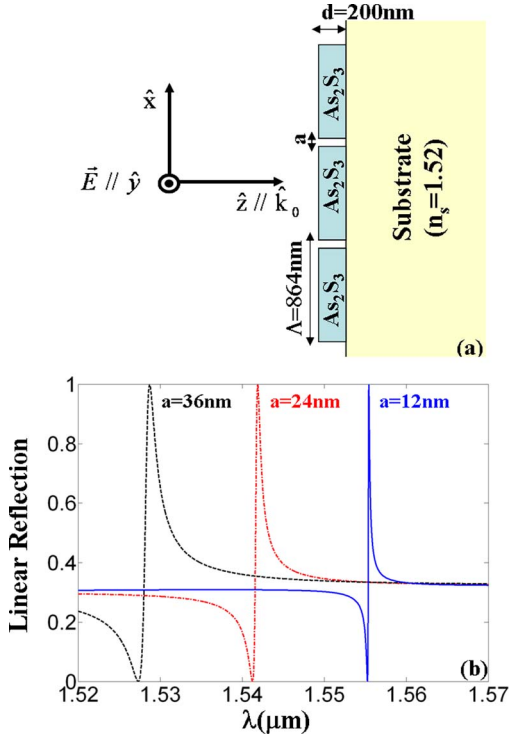

Fig. 1. (Color online) (a) As_2S_3 grating, thickness $d = 200$ nm, period $\Lambda = 864$ nm, and slit aperture a, grown on a glass substrate with $n_s = 1.52$. We consider an electromagnetic wave, TE-polarized at normal incidence. (b) Fano resonances in reflection for various slits' sizes. The Q factors of the resonances are, respectively, $Q \sim 7800$ for $a = 12$ nm, $Q \sim 2200$ for $a = 24$ nm, and $Q \sim 1000$ for $a = 36$ nm.

Report Documentation Page

Form Approved
OMB No. 0704-0188

1. REPORT DATE	2. REPORT TYPE	3. DATES COVERED
APR 2011		**00-00-2011 to 00-00-2011**

4. TITLE AND SUBTITLE	5a. CONTRACT NUMBER
All-optical switching at the Fano resonances in subwavelength gratings with very narrow slits	5b. GRANT NUMBER
	5c. PROGRAM ELEMENT NUMBER
6. AUTHOR(S)	5d. PROJECT NUMBER
	5e. TASK NUMBER
	5f. WORK UNIT NUMBER
7. PERFORMING ORGANIZATION NAME(S) AND ADDRESS(ES) **AEgis Technologies,Nanogenesis Division,410 Jan Davis Drive,Huntsville,AL,35806**	8. PERFORMING ORGANIZATION REPORT NUMBER
9. SPONSORING/MONITORING AGENCY NAME(S) AND ADDRESS(ES)	10. SPONSOR/MONITOR'S ACRONYM(S)
	11. SPONSOR/MONITOR'S REPORT NUMBER(S)

12. DISTRIBUTION/AVAILABILITY STATEMENT
Approved for public release; distribution unlimited

13. SUPPLEMENTARY NOTES

14. ABSTRACT

15. SUBJECT TERMS

16. SECURITY CLASSIFICATION OF:			17. LIMITATION OF ABSTRACT	18. NUMBER OF PAGES	19a. NAME OF RESPONSIBLE PERSON
a. REPORT **unclassified**	b. ABSTRACT **unclassified**	c. THIS PAGE **unclassified**	**Same as Report (SAR)**	**3**	

discussed in [12,13]. The excitation of the Fano resonances is mediated by the reciprocal lattice vectors of the grating as in a conventional grating coupler according to the following equation:

$$\sin(\vartheta) \cong \left| \pm n_{\mathrm{WG}} \mp m \frac{\lambda}{\Lambda} \right|, \qquad m = 0, 1, 2, \ldots, \qquad (1)$$

where ϑ is the incident angle, λ the incident wavelength, n_{WG} the real part of the effective index of the mode of the unperturbed waveguide (in our case the air/As_2S_3(200 nm)/substrate waveguide), Λ the grating period, and m the diffraction order. Equation (1) becomes exact as the slit aperture $a \to 0$, because in this case the grating structure gets closer and closer to the unperturbed waveguide. We have designed the grating so that at normal incidence and TE polarization it admits Fano resonances in the telecommunication band, i.e. between 1.52 and 1.56 μm, see Fig. 1(b). In particular, in our case the incident wavelength is approximately matched with the TE_0 guided mode of the unperturbed waveguide according to the equation $\lambda \cong n_{\mathrm{WG}}\Lambda$. Note that effective indexes of the unperturbed waveguide for the three resonances are, respectively, $n_{\mathrm{WG}} = 1.886$ at $\lambda = 1.5285$, $n_{\mathrm{WG}} = 1.881$ at $\lambda = 1.5419$, and $n_{\mathrm{WG}} = 1.875$ at $\lambda = 1.5555$, while the actual effective indexes of the resonances ($n_{\mathrm{eff}} = \lambda/\Lambda$) are, respectively, $n_{\mathrm{eff}} = 1.769$, $n_{\mathrm{eff}} = 1.7846$, and $n_{\mathrm{eff}} = 1.8003$. In other words, the actual position of the Fano resonances is slightly blueshifted with respect to what Eq. (1) predicts; moreover, the amount of the shift decreases as the grating approaches the uniform waveguide for narrower and narrower slits. In the calculations we have taken the dispersion of As_2S_3 by a linear interpolation of the experimental data tabulated in the book of Kloceck [14].

The reflection and transmission from the grating have been numerically calculated by using the Fourier modal method (FMM) [15]. Note that the quality (Q) factor ($Q = \lambda/\Delta\lambda$) of the resonances increases as the width a of the slits decreases; this is an expected phenomenon that can be explained by looking at these resonances as generated by leaky waveguide modes whose dwell time inside the As_2S_3 grating is longer and longer as the As_2S_3 grating becomes closer and closer to the unperturbed uniform layer. Such kinds of narrow resonances can still be easily resolved using pulses in the subnanosecond range (between 10 and 100 ps).

In Fig. 2 we show the onset of the optical bistability for the three resonances just described. The nonlinear calculation makes use of the FMM extended to deal with a cubic nonlinearity according to the mean field theory laid out in [7].

The nonlinear refractive index n_2 of As_2S_3 has been taken according to [5] equal to $2.9 \times 10^{-18}\ \mathrm{m^2/W}$ which corresponds to a cubic nonlinearity $\chi^{(3)} = 4.4 \times 10^{-20}\ \mathrm{m^2/V^2}$. This value of the cubic nonlinearity is almost 1 order of magnitude smaller than the value of a typical semiconductor material such like GaAs, but it is still 2 orders of magnitude greater than glass, for example.

The figures show how the onset of optical bistability is strictly linked to the Q factor of the resonances, as one may expect. In fact the high Q factor, or equivalently high density of modes, is an indication of the high local field

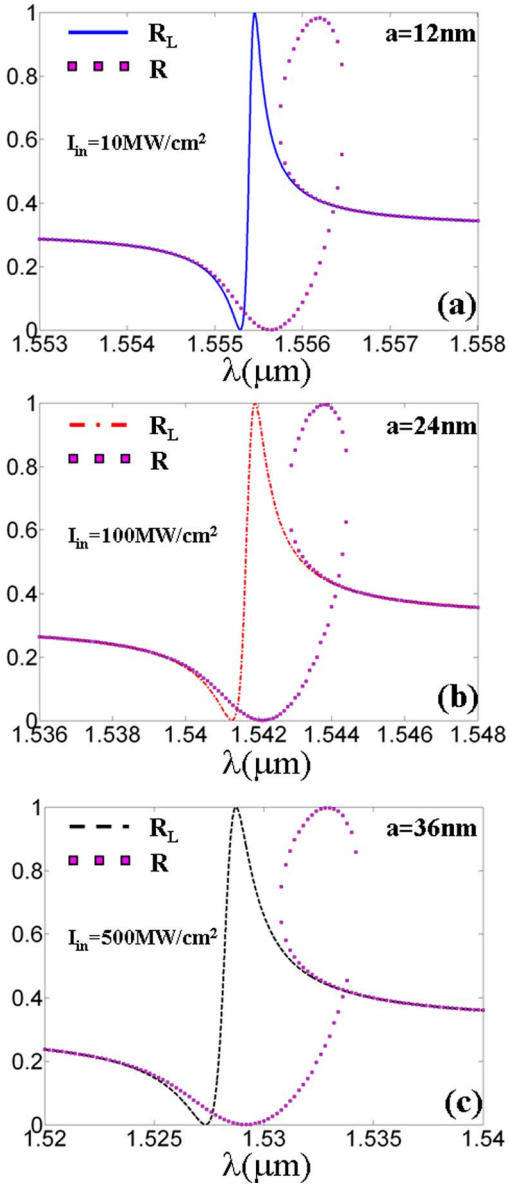

Fig. 2. (Color online) Linear reflection (R_L) and nonlinear reflection (R) with the onset of optical bistability at different values of the input intensity (I_{in}) for the three Fano resonances already described in Fig. 1(b).

intensity available inside the grating that fosters the inception of optical bistability at low input intensity. We note, in particular, how the input intensity for the start of the optical bistability roughly scales as $1/Q^2$ [see the Q factors of the corresponding linear resonances in the caption of Fig. 1(b)] in agreement with the scaling law reported in [16] for nonlinear photonic crystals with a Lorentzian line, for example.

In Fig. 3 we show the all-optical switching characteristics of the device. The operative wavelengths in the three cases have been chosen approximately at the center of the optical bistability region (see Fig. 2). The fact that the two stable branches have a crossing point should not be considered a problem. In fact, for continuity reasons, the nonlinear reflection simply follows the stable branch 1 until the switching point S1 for increasing input intensities and follows the stable branch 2 until the switching point S2 for decreasing input intensities.

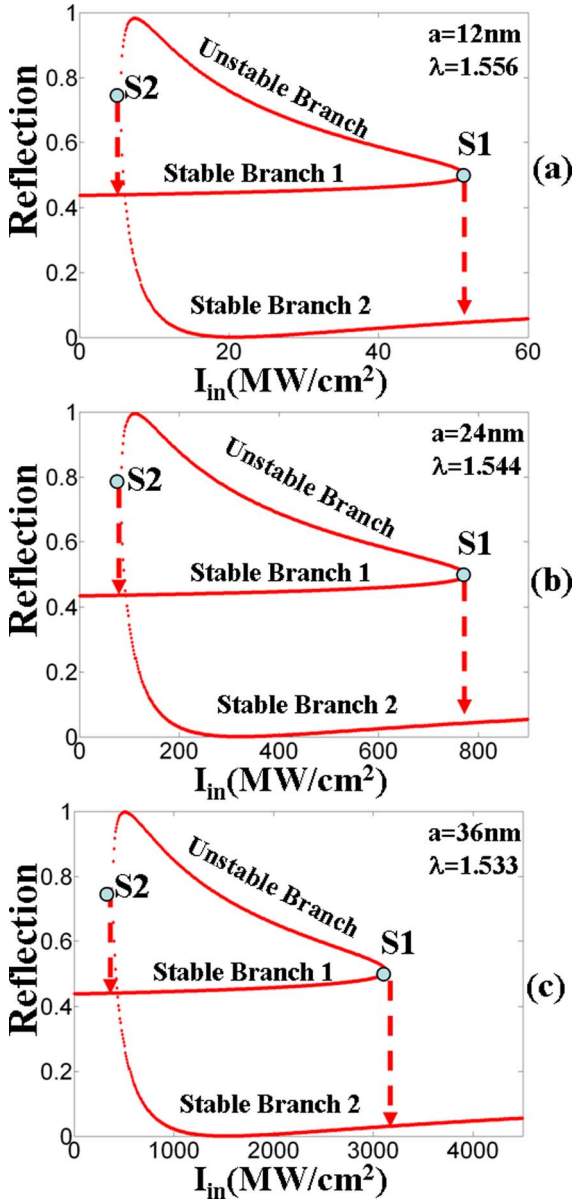

Fig. 3. (Color online) Reflection versus input intensity (I_{in}) at different incident wavelengths for the three cases. The dots indicated with S1 and S2 and the corresponding dashed arrows represent, respectively, the switching points of the transition from the stable branch 1 to stable branch 2 (S1) for increasing input intensity and from stable branch 2 to stable branch 1 (S2) for decreasing input intensity.

It is worthwhile to draw attention once again to the critical role played by the slits aperture in decreasing the switching threshold of the device. The switching threshold can be decreased of nearly 2 orders of magnitude by decreasing the slit's size from $a = 36\,\mathrm{nm}$ [Fig. 3(c)] to $a = 12\,\mathrm{nm}$ [Fig. 3(a)]. Also in this case the $1/Q^2$ dependence of the switching intensity can easily be ascertained. It is opportune at this point to mention that thermally evaporated As_2S_3 thin films have been found to be photosensitive at telecommunication wavelengths, unlike their bulk counterpart, for local intensities $\sim 1\,\mathrm{GW/cm^2}$ and long exposure times [17]. While an improvement in deposition techniques may eventually lead to As_2S_3 thin films that have the same stability as the corresponding bulk material, nevertheless we would like to comment on the generality of our approach that does not rely in particular on the use of chalcogenide glasses but can be in principle applied to any diffraction grating provided that the material possesses low TPA. In our case the peak intensity in the glass at the switching point S1 is $\sim 15\,\mathrm{GW/cm^2}$ for Fig. 3(a), $\sim 60\,\mathrm{GW/cm^2}$ for Fig. 3(b), and $\sim 120\,\mathrm{GW/cm^2}$ for Fig. 3(c). If, for example, we have a grating with a 6 nm slit, peak intensity in the glass well below $10\,\mathrm{GW/cm^2}$ can be expected. Photostable thin film chalcogenide glasses with optical damage threshold $\sim 35\,\mathrm{GW/cm^2}$ have been recently reported [18]. Given the dramatic improvements in current nanofabrication techniques [8] and in the processing of chalcogenide glasses [18], we believe that the results presented here may pave the way for a new class of efficient all-optical switching devices at telecommunication wavelengths.

References and Notes

1. H. M. Gibbs, *Optical Bistability: Controlling Light with Light* (Academic, 1985).
2. Here we suppose to write the relative permittivity of the medium as $\varepsilon = \varepsilon_L + \chi^{(3)}|E|^2$ and the intensity as $I = (1/2)\varepsilon_0 c n_L |E|^2$. Other conventions also exist where $\varepsilon = \varepsilon_L + 3\chi^{(3)}|E|^2$ and $I = 2\varepsilon_0 c n_L |E|^2$, in this case we would have had that $\mathrm{Re}[\chi^{(3)}] = 4\varepsilon_0 c n_L^2 n_2/3$ and $\mathrm{Im}[\chi^{(3)}] = \frac{\varepsilon_0 c n_L^2 \lambda}{3\pi}\beta$. See, for example, R. L. Sutherland, *Handbook of Nonlinear Optics* (Marcel Dekker, 1996).
3. V. Mizrahi, K. W. DeLong, and G. I. Stegeman, Opt. Lett. **14**, 1140 (1989).
4. W. C. Hurlbut, Yun-Shik Lee, K. L. Vodopyanov, P. S. Kuo, and M. M. Fejer, Opt. Lett. **32**, 668 (2007).
5. V. Ta'eed, N. J. Baker, L. Fu, K. Finsterbusch, M. R. E. Lamont, D. J. Moss, H. C. Nguyen, B. J. Eggleton, D. Y. Choi, S. Madden, and B. Luther-Davis, Opt. Express **15**, 9205 (2007) and references therein.
6. U. Fano, Phys. Rev. **124**, 1866 (1961).
7. P. Vicent, N. Paraire, M. Neviere, A. Koster, and R. Reinisch, J. Opt. Soc. Am. B **2**, 1106 (1985).
8. H. Duan, D. Winston, J. K. W. Yang, B. M. Cord, V. R. Manfrinato, and K. K. Berggren, J. Vac. Sci. Technol. B **28**, C6 (2010) and references therein.
9. A. E. Miroshnichenko, S. Flach, and Y. S. Kivshar, Rev. Mod. Phys. **82**, 2257 (2010) and references therein.
10. B. Luk'yanchuck, N. I. Zheludev, S. A. Maier, N. J. Halas, P. Nordlander, H. Giessen, and C. T. Chong, Nat. Mater. **9**, 707 (2010) and references therein
11. C. Grillet, D. Freeman, B. Luther-Davis, S. Madden, R. McPhedran, D. J. Moss, M. J. Steel, and B. J. Eggleton, Opt. Express **14**, 369 (2006).
12. G. D'Aguanno, N. Mattiucci, M. J. Bloemer, D. de Ceglia, M. A. Vincenti, and A. Alù, J. Opt. Soc. Am. B **28**, 253 (2011).
13. D. de Ceglia, G. D'Aguanno, N. Mattiucci, M. A. Vincenti, and M. Scalora, Opt. Lett. **36**, 704 (2011).
14. P. Klocek, *Handbook of Infrared Optical Materials* (Marcel Dekker, 1991)
15. L. Li, J. Opt. Soc. Am. A **13**, 1870 (1996) and references therein.
16. M. Soljacic, M. Ibanescu, C. Luo, S. G. Johnson, S. Fan, Y. Fink, and J. D. Joannopoulos, Proc. SPIE **5000** 200 (2003).
17. N. Hô, J. M. Laniel, R. Valée, and A. Villeneuve, Opt. Lett. **28**, 965 (2003).
18. P. Němec, S. Zhang, V. Nazabal, K. Fedus, G. Boudebs, A. Moreac, M. Cathelinaud, and X.-H. Zhang, Opt. Express **18**, 22944 (2010).